Optimization of Influential Parameters for the Degradation of Metronidazole Contained in Aquaculture Effluent via Sonocatalytic Process: Kinetics and Mechanism

O.H. Aremu*†, C.O. Akintayo*, S.M. Nelana**, M.J. Klink** and O.S. Ayanda*

*Department of Industrial Chemistry, Federal University Oye-Ekiti, PMB 373, Oye-Ekiti, Nigeria
**Department of Chemistry, Vaal University of Technology, Vanderbijlpark, South Africa
†Corresponding author: O.H. Aremu; omololaaremu21@gmail.com

ABSTRACT

This study examined the synthesis of a viable catalyst for the degradation of metronidazole contained in aquaculture effluent. Zinc oxide nanoparticles (n-ZnO) were synthesized via the precipitation method and calcined at 500°C in a muffle furnace to enhance the degradability properties. The morphology showed a hexagonal structure with an average particle size of 71.48 nm and the elemental composition showed a higher weight percent of 59.15% for zinc and 21.65% for oxygen. The FTIR confirms the vibrational characteristic mode of the Zn-O band at 427.21cm^{-1}. The XRD showed a good crystallinity and the BET surface area was 8.58 m^2.g^{-1} which showed that the n-ZnO possesses more active sites that can remove pollutants from wastewater. However, no studies have been done on the removal of MNZ in aquaculture effluent. The kinetics followed pseudo-second-order kinetics and the Langmuir-Hinshelwood model best fit the degradation process with R^2, Kc, and K$_{LH}$ values of 0.96781, 1.486 × 10^{-1} mg. Lmin^{-1}) and 8.790 × 10^{-2} (L.mg^{-1}). Under the influential parameters, the percentage COD removal achieved for MNZ in aquaculture effluent was 62.6%, 89.8%, and 98.5% of MNZ at 20% ultrasonic amplitude, 5 mL 2% H$_2$O$_2$ and 0.02g n-ZnO within 60 min sonication time for US only, US/n-ZnO and US/n-ZnO/H$_2$O$_2$ systems. Hence, MNZ contained in aquaculture effluent can best be degraded with the synergetic effect of the US/n-ZnO/H$_2$O$_2$ system.

INTRODUCTION

Pharmaceuticals and personal care products are evolving aquatic pollutants that are on the increase in the environment due to their active use (Calamari et al. 2003). The stored-up pharmaceuticals in the aquatic environment find their way via wastewater treatment plants, sewage sludge, pharmaceutical industries, and households (Petrie et al. 2015) as a result of extreme applications by humans (Felis et al. 2020). Almost 95% of pharmaceuticals are discharged from the body into the environment which has a toxic impact on the ecosystem (Habibi et al. 2018, Jury et al. 2010). Generally, antibiotics are used as feed condiments, growth promoters (Manyi-Loh et al. 2018), and therapeutics in the production of livestock and aquatic animals (Landers et al. 2012).
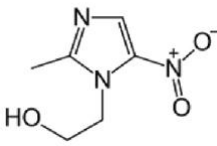
Metronidazole (MNZ) is one of the antibiotics consumed for the treatment of infections. It belongs to the class of compound nitroimidazole, it is used to treat infections caused by bacteria and protozoa. It is active against *Trichomonas vaginalis* and *Balantadium coli* (Das & Dhua 2014). The high solubility and stability of metronidazole in water have

led to its availability in the environment, non-biodegradability, and contribution to environmental pollution as a result of its excessive use (Yang et al. 2019). The buildup of metronidazole in the body is capable of leading to cancer and mutations which invariably promotes toxic substances in the body system and when metabolism takes place, the environment becomes toxic (Cunningham 2004). Table 1 shows the properties of metronidazole.

The solubility of MNZ has made it difficult to be removed it from the aquatic environment via conventional treatment and activated carbon (Forouzesh et al. 2018). Advanced oxidation processes (AOPs) are innovative technologically in the treatment of wastewater through the generation of hydroxyl radicals that are capable of removing organic contaminants. AOPs have been integrated using ozonation, photocatalysis (Balarak et al. 2019), sono-Fenton, and electrochemical oxidation in the removal of MNZ in the aquatic environment.

Ultrasound is one of the advanced oxidation processes (AOPs) and is a technique that employs the generation of hydroxyl radicals that attacks the pollutants and mineralize to

Table 1: Properties of Metronidazole.

Structure	
Physical State	Crystalline solid powder
Molecular formulae	$C_6H_9N_3O_3$
Class	Nitroimidazole
Molecular weight	171.15 g.mol^{-1}
Boiling point	405.4^{o}C
Melting point	158-160°C
Synonyms	Flagyl
Color	White to pale yellow
Solubility	1g in 100 mL of water @ 20°C
Stability	Stable in air

CO_2 and H_2O. Hydroxyl radicals (OH) are powerful oxidants that do not produce secondary pollutants. Acoustic cavitation is the mechanism that ultrasound operates on; it involves the production of cavitation bubbles through sound energy at increased temperature and pressure which leads to the invention of active chemical oxidants (Ayanda et al. 2021).

Among all metal oxide catalysts, ZnO nanoparticles have proven to be as good catalysts due to their photocatalytic capacity, non-toxic nature, antimicrobial properties, the enlarged band gap of 3.37 eV, increased binding energy of 60 meV, easy synthesis, piezo and pyro-electric properties (Bian et al. 2017) have increased its wider applications. Different methods have been explored in the synthesis of zinc oxide nanoparticles, methods such as ultrasound, hydrothermal, green synthesis, electrochemical, precipitation, microwave, sol-gel, and chemical vapor deposition (Aremu et al. 2021). Studies have shown that there are fewer reports on the removal of metronidazole in aquaculture effluent using ultrasound, ultrasound/ H_2O_2, ultrasound/ZnO, and ultrasound/ZnO/ H_2O_2 systems.

Hence, the objective of this research is to synthesize a non-toxic ZnO nanoparticle calcined at 500°C, characterize, and optimize the influential parameters on the degradation of metronidazole contained in aquaculture effluent via sonocatalytic process, and study the kinetics and mechanism

MATERIALS AND METHODS

Chemicals and Reagents

Metronidazole (MNZ) of 97% purity, $ZnCl_2$, NaOH, and H_2O_2 were purchased from Sigma Aldrich, USA. A 50 mg.L^{-1}

of MNZ solution was prepared for the stock solution. Various working solutions were prepared from the stock solution. A pH meter (PHS-3C) was used to regulate the MNZ solution contained in the wastewater by adding 0.05M HCl or 0.05M NaOH solutions.

Synthesis of n-ZnO

A 20 g of $ZnCl_2$ was weighed into 100 mL of de-ionized water in a 250 mL beaker. It was continuously stirred at a temperature of 90°C for 20 min with a magnetic stirrer. 50 mL of the $ZnCl_2$ solution was added to 0.6 M NaOH solution. The resultant mixture was filtered with a Whatman filter paper and washed thrice with deionized water to obtain the ZnO nanoparticles. The filtered sample was oven dried for 24 h at 75°C, calcined for 2 h in a muffle furnace at 500°C, and crushed to obtain fine ZnO nanoparticles.

Characterization of n-ZnO

The morphology of the ZnO nanoparticles was examined using a scanning electron microscope (SEM; Phenon type Model: Pro X) and transmission electron microscope (TEM; Tecnai G^2 20) at 100 nm. The elemental composition of the n-ZnO was quantitatively determined by electron dispersive spectroscopy (EDS), the crystallinity was investigated with X-ray diffraction (Siemens D8 Advance Bruker XRD) with CuK∞ radiation, the functional group was investigated with Fourier Transform Infrared Spectroscopy (FTIR; Perkin Elmer Spectrum Two ^{TM} Spectrometer) and the Brunauer Emmett and Teller (BET) surface area was investigated by a Tristar 3000 analyzer with N_2 adsorption at -196°C.

Removal of MNZ

The removal of MNZ was investigated with ultrasound (US), US/n-ZnO, and a combined US/n-ZnO/H_2O_2 system. respectively. At the end of the removal process, samples were taken and analyzed with a UV-visible spectrophotometer at a wavelength of 320 nm.

Ultrasound

Influence of ultrasonic amplitude and sonication time on the removal of MNZ: Using different ultrasonic amplitudes (20-100%) and an ultrasonic frequency of 20 kHz, 50 mL of a 50 mg.L^{-1} MNZ aqueous solution was processed in a 200 mL reactor for 20 to 60 minutes.

Influence of H_2O_2 concentration and sonication time on the removal of MNZ: 5 mL of 1%, 2%, and 4% of H_2O_2 were added in a 50 mL MNZ solution at varying sonication times (20-60 min), 60 % ultrasonic amplitude, and a frequency of 20 kHz.

Influence of initial concentration of MNZ and sonication time on the removal of MNZ: The influence of varying concentrations (3.125 mg.L^{-1}-50 mg.L^{-1}) was examined at sonication times (20-60 min), 60 % ultrasonic amplitude, and a frequency of 20 kHz.

Influence of pH and sonication time on the removal of MNZ: The influence of varying pH (2-10) was examined at sonication times (20-60 min), 60% amplitude, and a frequency of 20 kHz.

Ultrasound/n-ZnO

Influence of ultrasonic amplitude and sonication time on the removal of MNZ: A 0.02 g of n-ZnO was added to 50 mL of 50 mg.L^{-1} MNZ aqueous solution, sonicated at varying sonication times (20-60 min) and a frequency of 20 kHz.

Influence of nanodosage and sonication time on the removal of MNZ: 50 mL of 50 mg.L^{-1} MNZ aqueous solution with the addition of 0.02–0.10 g of ZnO nanoparticles in a 200 mL reactor at an ultrasonic amplitude of 60% and ultrasonic frequency of 20 kHz within 20-60 mins.

Influence of initial concentration and sonication time on the removal of MNZ: A 0.06 g of n-ZnO was added to each of the varying concentrations of 50 mL of 50 mg.L^{-1} MNZ aqueous solution at varying sonication times (20-60 min), 60% ultrasonic amplitude, and a frequency of 20 kHz.

Influence of pH and sonication time on the removal of MNZ: A 0.06 g of n-ZnO was added to each of the varying pH of 50 mL of 50 mg.L^{-1} MNZ aqueous solution, sonicated at varying sonication times (20-60 min), 60% ultrasonic amplitude and a frequency of 20 kHz.

Influence of H_2O_2 concentration and sonication time on the removal of MNZ: A 0.06 g of n-ZnO was added to each of the varying H_2O_2 concentrations of 50 mL of 50 mg.L^{-1} MNZ aqueous solution at varying sonication times (20-60 min), 60% ultrasonic amplitude, and a frequency of 20 kHz.

Ultrasound/n-ZnO/H_2O_2

Influence of ultrasonic amplitude and sonication time on the removal of MNZ: A 0.06 g of n-ZnO and 5 mL of 1% H_2O_2 were added to each of the varying amplitudes of 50 mL of 50 mg/L MNZ aqueous solution, sonicated at varying sonication times (20-60 min) and a frequency of 20 kHz.

Influence of nanodosage and sonication time on the removal of MNZ: 5 mL of 1% H_2O_2 and each of 0.02-1.0 g of n-ZnO were added to 50 mL of 50 mg.L^{-1} MNZ aqueous solution, sonicated at varying sonication time (20-60 min), 40% ultrasonic amplitude, and a frequency of 20 kHz.

Influence of initial concentration of MNZ and sonication time on the removal of MNZ: A 0.08 g of n-ZnO and 5 mL of 1% H_2O_2 were added to 50 mL of each of the varying concentrations, sonicated at varying sonication times (20-60 min), 40% ultrasonic amplitude, and a frequency of 20 kHz.

Influence of pH and sonication time on the removal of MNZ: A 0.08 g of n-ZnO and 5 mL of 1% H_2O_2 were added to 50mL of 50 mg.L^{-1} MNZ aqueous solution, sonicated at varying sonication times (20-60 min), 40% ultrasonic amplitude and a frequency of 20 kHz. The percentage removal of MNZ was calculated using Eq. (1)

$$\% \text{ Degradation} = \frac{(MNZ)_0 - (MNZ)_e}{(MNZ)_0} \times 100 \qquad \ldots (1)$$

Where MNZ_0 and MNZ_e are the initial and final concentrations of MNZ respectively.

Application of influential parameters to aquaculture effluent: The influential parameters such as the dosage of ZnO nanoparticles, sonication time, ultrasonic amplitude, H_2O_2 concentration, and ultrasonic frequency were introduced to aquaculture effluent. A 50 mL of the aquaculture effluent was spiked with MNZ.

RESULTS AND DISCUSSION

Characterization

The SEM and TEM analyses of the calcined (500°C) ZnO nanoparticles formed from 0.6 M NaOH at 20.0 kx magnification, scaled at 2 μm, and shot at 100 nm are presented in Figs. 1a and 2a respectively. It was observed that more prominent pores with multiple hexagonal structures in mass were depicted (Mallika et al. 2015). The EDS spectrum of the synthesized n-ZnO calcined at 500°C

formed in 0.6 M NaOH are in proportion 17.93±4.9wt% C, 21.65±7.2wt% O, 1.27±0.4 wt% Cl, and 59.15±11.3wt% Zn is shown in Fig. 1b. The result showed that as the Cl decreases, the percentage of Zn increases which indicates that ZnO nanoparticles were synthesized. The presence of Cl was due to the precursor used during synthesis. The particle size distribution of ZnO nanoparticles was examined by subjecting the TEM micrographs to image J software to measure the diameter of particles and this is presented in Fig. 2b. The result showed that the average particle size was 71.48 nm. The plots of N_2 adsorption-desorption isotherm and Barret-Joyner-Halenda (BJH) pore size distribution of ZnO nanoparticles formed in 0.6 M NaOH, calcined at 500^0C are presented in Fig.3a and 3b. The result shows that surface area, pore volume, and pore size were 8.5808 $m^2.g^{-1}$, 0.038 $cm^3.g^{-1}$, and 164.177 A^0 (Kołodziejczak-Radzimska et al. 2012). The hysteresis loop resembles type IV which is in line with the IUPAC classification (Ismail et al. 2018).

The FTIR spectrum of ZnO nanoparticles calcined at 500^0C indicates an absorption band at 467.21 cm^{-1} which corresponds to the vibrational mode of the Zn-O bond (Zak et al. 2011) as shown in Fig 4.

The X-ray diffractograms shown in Fig. 5 depict the hexagonal nature of ZnO nanoparticles as a result of its complete crystallinity with the highest peak at (101) plane which corresponds to the report of Saif-Aldin et al. (2020). The average crystallite size was calculated using the De-bye Scherrer equation in Eq. 2

$$D= K\lambda / (\beta \cos\Theta) \qquad …(2)$$

Where D is the crystallite size in nm, K is a constant (0.9), λ is the wavelength (1.54060 A^0), Θ is the Bragg's angle and β is the Full Width at Half Maximum (FWHM). The average crystallite size of the annealed ZnO nanoparticles at 500^0C was 72.01 nm (Kayani et al. 2015) which corresponds to the particle size obtained from the TEM micrograph analysis.
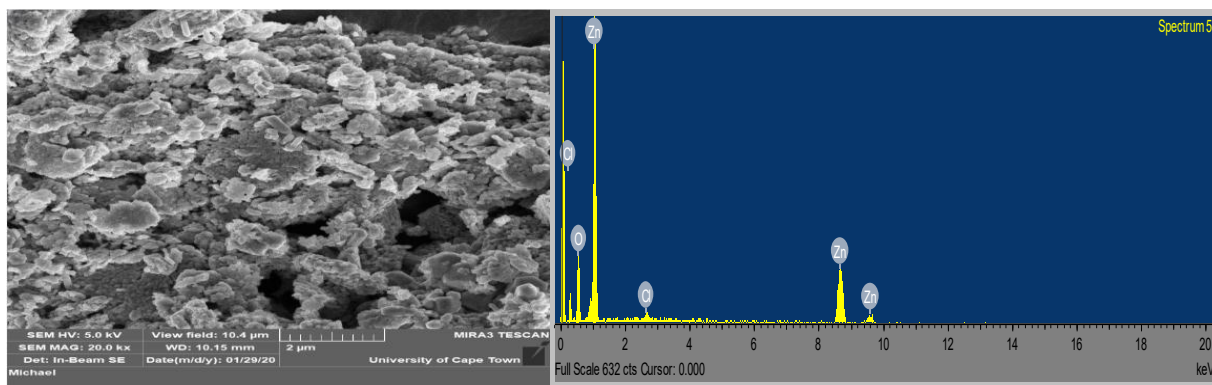

Fig. 1 (a) and (b): SEM-EDS of the ZnO calcined at 500°C formed in 0.6M NaOH.
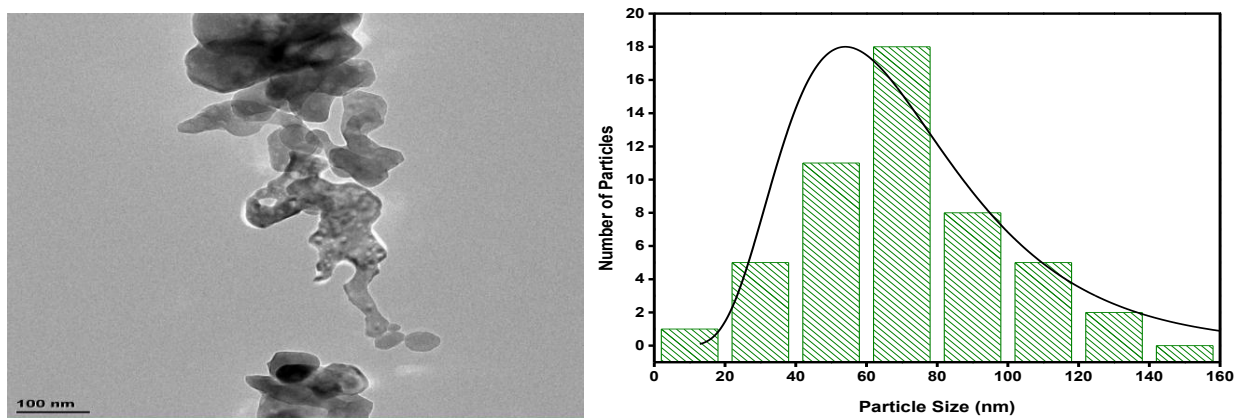

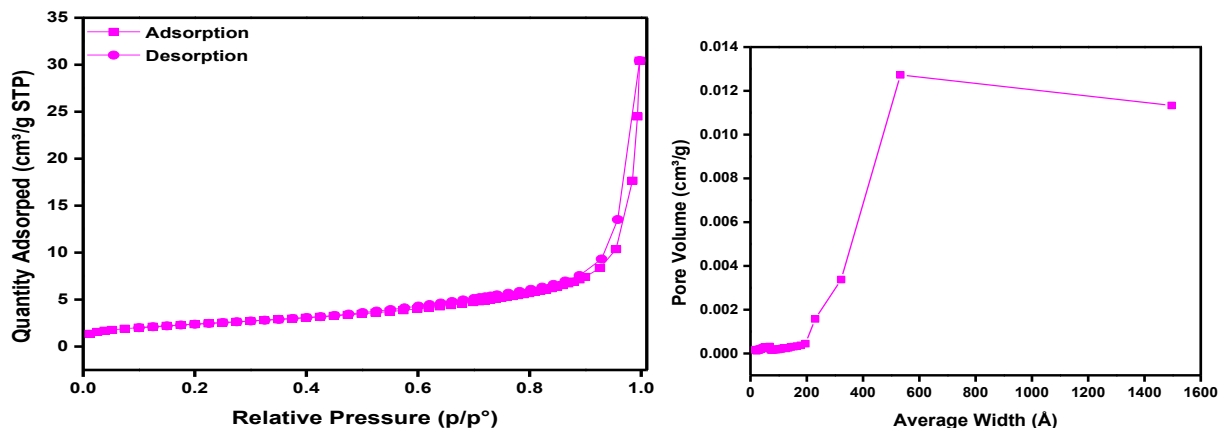Fig. 2: TEM micrographs (a) and particle size distribution (b) of the calcined ZnO nanoparticles at 500°C.

Figs 3: N$_2$ adsorption-desorption isotherm (a) and Barret-Joyner-Halenda (BJH) pore size (b) distribution of n-ZnO calcined at 500°C.

Removal of MNZ

Influence of ultrasonic amplitude and sonication time on the removal of MNZ: Fig. 6 showed that the maximum degradation of MNZ was achieved at 60% ultrasonic ampli-
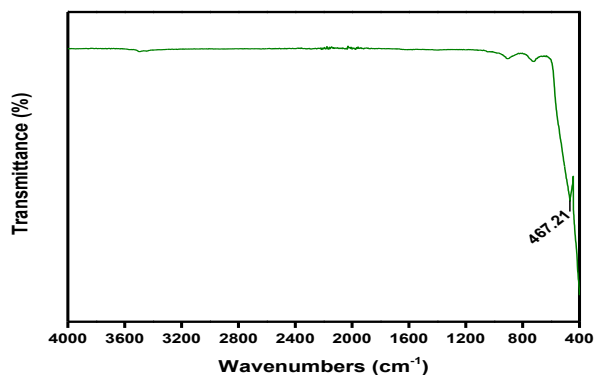

Fig. 4: The FTIR spectrum of ZnO nanoparticles calcined at 500°C.

Fig. 5: The XRD of ZnO nanoparticles calcined at 500°C.

tude with values 30.3%, 33.3%, 36.7%, 38.3%, and 41.2% within 20-60 min sonication time. It was observed that the degradation of MNZ increases as sonication time increases. From the data presented, ultrasound alone is not sufficient for MNZ degradation. A 60% ultrasonic amplitude was kept constant for further experiments.

Influence of H$_2$O$_2$ concentration and sonication time on MNZ degradation: The maximum removal of MNZ was achieved at a higher concentration of H$_2$O$_2$ (4%) with percentage degradation of 83.5%, 85.6%, 87.4%, 88.5%, and 89.8% within 20-60 min sonication time in Fig. 7. This implies that increase in H$_2$O$_2$ concentration is dependent on MNZ removal as more hydroxyl radicals were available to remove MNZ.

Influence of initial concentration and sonication time on MNZ degradation: The result in Fig. 8 shows that as the concentration of MNZ reduces, the degradation rate in-
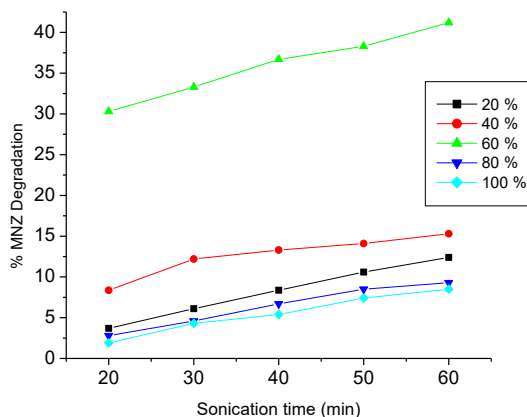

Fig. 6: Influence of ultrasonic amplitude and sonication time on MNZ removal.

creases. The maximum degradation of MNZ was achieved at 3.125 mg.L^{-1} within 20-60 min sonication time and 60% ultrasonic amplitude with percentage degradation of 58.8%, 61.1%, 62.2%, 64.1%, and 65.6%. This implies that better degradation of MNZ can be achieved at lower concentrations and this may be due to the flooding of more MNZ molecules in solution that is capable of reducing the reactive species in the ultrasonic reactor (Cordero et al. 2007). In the same vein, the kinetic studies follow a pseudo-second-order reaction which is shown in Fig. 9.

Influence of pH and sonication time on MNZ removal: The pH of a solution has an effect on the ionization of contaminants and the charges on the surface of adsorbents. The result in Fig. 10 showed that the maximum removal was achieved at an acidic medium. This implies that the availability of more protons at higher pH to attack the pollutants will increase the degradation rate. The percentage removal

achieved were 67.4%, 68.5%, 69.5%, 70.6% and 71.7% at pH 2 (Hemati Borji et al. 2010).

Ultrasound/n-ZnO

Influence of ultrasonic amplitude and sonication time on MNZ removal: A 0.02 g n-ZnO was added to 50 mg.L^{-1} MNZ solution and sonicated within 20-60 min at varying ultrasonic amplitude (20-100%). Fig. 11 shows that the maximum removal was achieved at 60% ultrasonic amplitude. The percentage removal achieved was 42%, 44.9%, 46.2%, 48%, and 50.9% which is higher than that of the US alone. This implies that more active sites were available from the catalyst to mineralize pollutants and also the OH radicals produced from ultrasound have led to a major increase in the removal process (Qiao et al. 2018). A 60% ultrasonic amplitude was kept constant for further experiments.
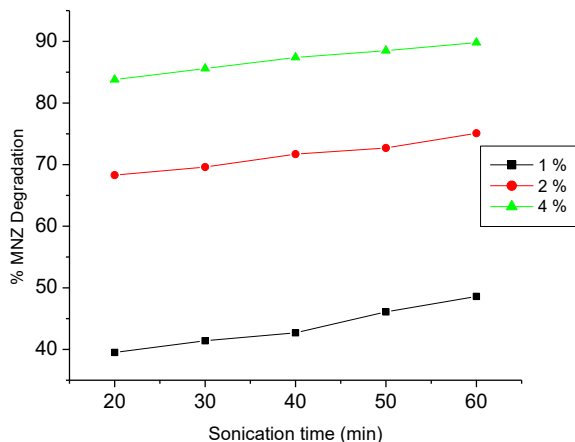

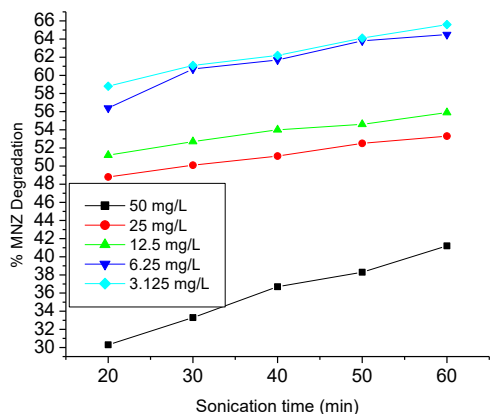Fig.7: Influence of H$_2$O$_2$ concentration and sonication time on MNZ removal.

Fig. 9: Plot of 1/ (MNZ$_t$) and sonication time for pseudo-second-order kinetic model.

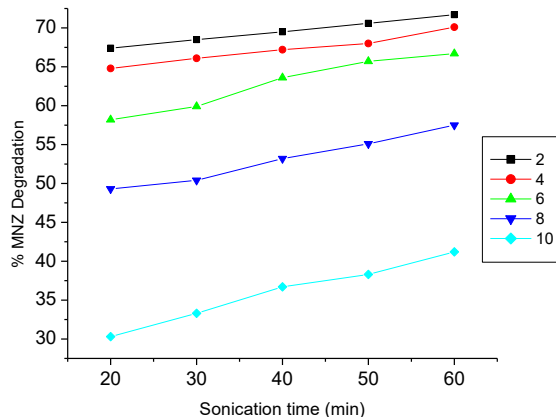Fig. 8: Influence of initial concentration and sonication time on MNZ degradation.
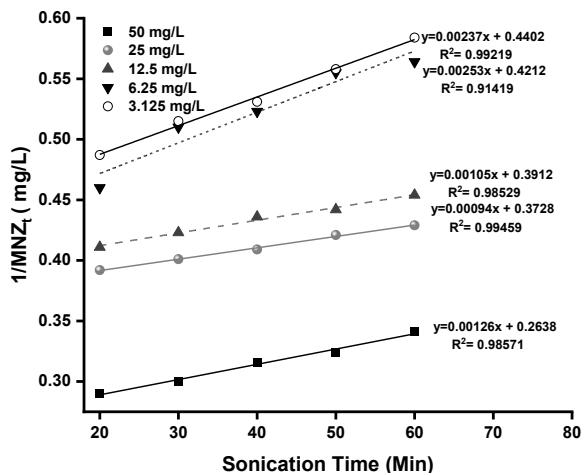
Fig. 10: Influence of pH and sonication time on MNZ degradation.

Influence of nanodosage and sonication time on MNZ removal: The result in Fig. 12 showed that a higher quantity of n-ZnO is not dependent on MNZ removal. The maximum MNZ removal achieved at 0.02g n-ZnO was 50.9% within 60 min sonication time. It was observed that as the quantity of n-ZnO increases, the removal of MNZ decreases which may be a result of insufficient surface area due to the agglomeration nature of n-ZnO (El Bouraie & Ibrahim 2020). Increasing n-ZnO in MNZ removal showed that the active sites are saturated and so there was no room for attacking pollutants. A 0.02g n-ZnO was kept constant for further experiments.

Influence of initial concentration and sonication time on MNZ removal: The maximum percentage removal shown in Fig. 13 follows the trend 68.2%, 70.6%, 71.9%, 73.7% and 75.1% at 3.125 mg.L^{-1} within 20-60 min. Increasing the concentration of MNZ may lead to saturation of active sites of the adsorbent thereby reducing the degradation efficiency
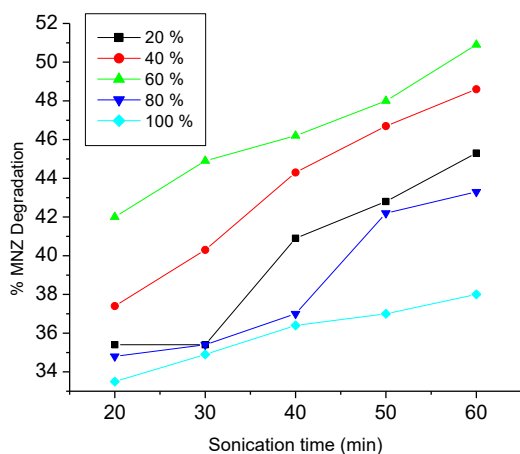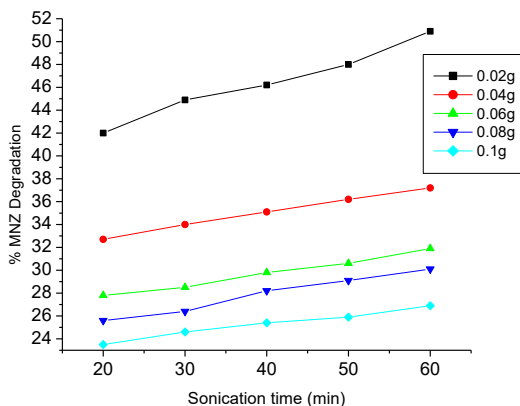
(Moussavi et al. 2013). The synergetic effect of US/n-ZnO is a viable technique for removing MNZ in an aqueous solution. In the same vein, the kinetic studies follow a pseudo-second-order reaction which is shown in Fig. 14.

Influence of pH and sonication time on MNZ removal: The initial pH of MNZ was 9.2. The maximum removal of MNZ was achieved at pH 2 with a percentage degradation of 79.5% within 60 min in Fig. 15. The combination of the protons from the adsorbate and the active sites of n-ZnO has improved the degradation rate from 71.9-79.5% within 20-60 min (El-Kemary et al. 2010).

Influence of H$_2$O$_2$ concentration and sonication time on MNZ removal: The result in Fig. 16 showed that the maximum removal of MNZ achieved at 2% H$_2$O$_2$ was 94% within 60 min. It was observed that the removal of MNZ increases with time. Increasing the concentration of H$_2$O$_2$ may disrupt the removal process.
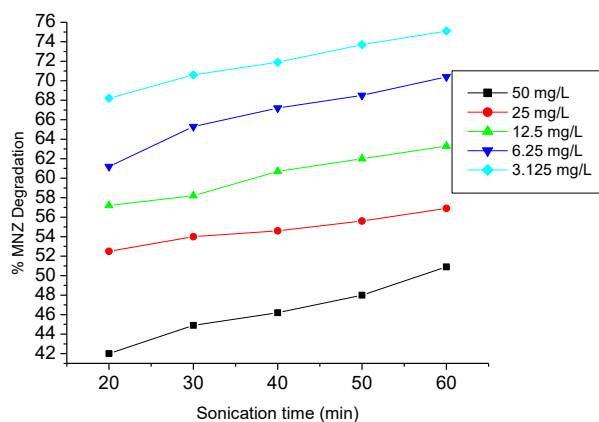

Fig. 11: Influence of ultrasonic amplitude and sonication time on MNZ removal.

Fig. 13: Influence of initial concentration and sonication time on MNZ removal.

Fig. 12: Influence of nanodosage and sonication time on MNZ removal.
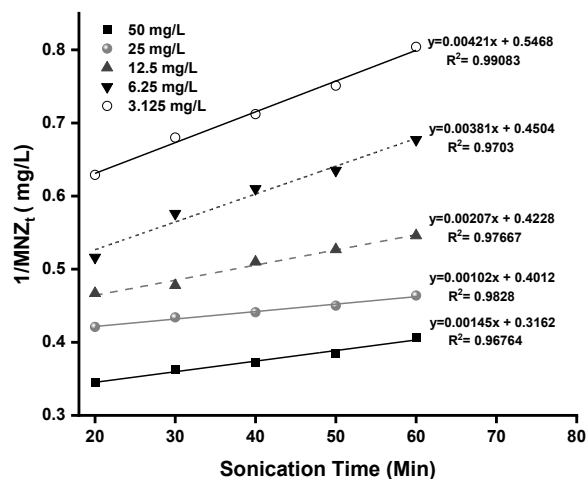

Fig. 14: Plot of 1/ (MNZ$_t$) and sonication time for pseudo-second-order kinetic model.

US/n-ZnO/ H$_2$O$_2$

Influence of ultrasonic amplitude and sonication time on MNZ removal: A 5 mL of 2% H$_2$O$_2$, 0.02 g n-ZnO were added to 50 mg.L^{-1} MNZ solution within 20-60 min sonication time. The result in Fig. 17 showed that the removal of MNZ increases with time from 63.8%-69.3% within 60 min at 20% ultrasonic amplitude. Increasing ultrasonic amplitude led to a decrease in the removal rate. This implies that amplitude is not dependent on MNZ removal. The synergetic influence of US/n-ZnO/ H$_2$O$_2$ on the removal of MNZ yielded a better removal when compared to US/n-ZnO and US alone. A 20% amplitude was kept constant for further experiments.

Influence of nanodosage and sonication time on MNZ removal: A 0.02-0.1 g n-ZnO were investigated with US/n-ZnO/ H$_2$O$_2$ system in 50 mg.L^{-1} MNZ solution with 5 mL 2% H$_2$O$_2$ at 20% ultrasonic amplitude. The result in Fig. 18 showed that the maximum removal of 69.3% was achieved at 0.02 g n-ZnO within 60 min. this implies that the removal

of MNZ increases with time and increasing the amount of n-ZnO may lead to saturation of active sites of the adsorbent (Sharifpour et al. 2018). A 0.02 g n-ZnO was kept constant for further experiments.

Influence of pH and sonication time on MNZ removal: The result in Fig. 19 showed that the removal of MNZ favors the basic medium (pH10) as more OH radicals will be available for the mineralization of MNZ (Malakootian et al. 2019). It was also observed that the removal of MNZ increases with time from 63.8-69.3% within 60 min sonication time.

Influence of initial concentration and sonication time on MNZ removal: The result in Fig. 20 showed that the removal of MNZ increases with decreasing concentration of MNZ. The maximum removal of MNZ was achieved at 3.125 mg.L^{-1} within 20-60 min. the percentage removal increases from 81.1%-88%. This implies that at lower concentrations of MNZ, excess OH radicals are available for the removal process (Ayanda et al. 2021).
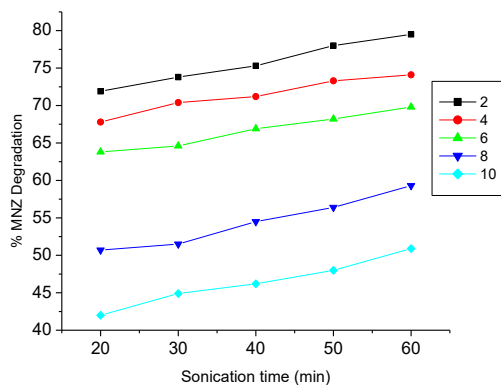

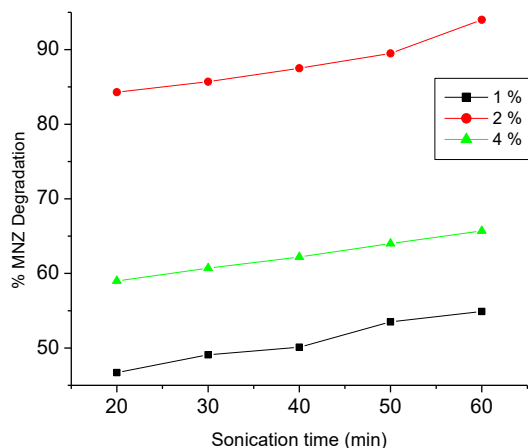Fig. 15: Influence of pH and sonication time on MNZ removal.

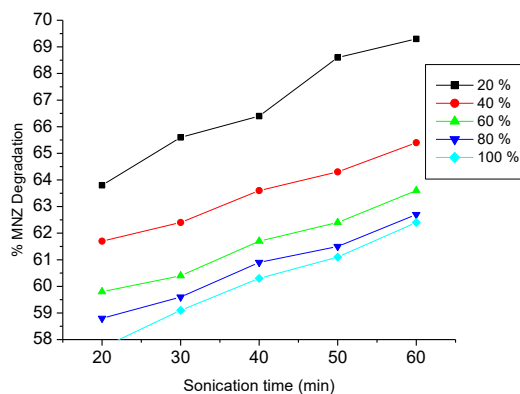Fig. 17: Influence of H$_2$O$_2$ concentration and sonication time on MNZ removal.

Fig. 16: Influence of H$_2$O$_2$ concentration and sonication time on MNZ removal.
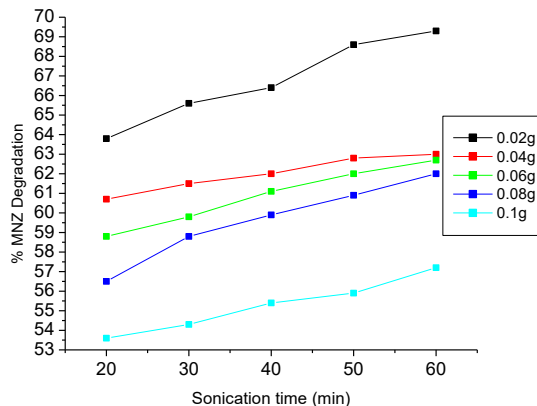

Fig. 18: Influence of nanodosage and sonication time on MNZ removal.

From the experimental data above, the influence of initial concentration was subjected to a pseudo-second-order kinetic model presented in Eq. (3)

$$\frac{1}{MNZ_t} = K_{obs}t \qquad \ldots(3)$$

Where MNZ_t is the final concentration of MNZ solution $(mg.L^{-1})$, K_{obs} is the observed rate of degradation and t is the time. The plot of $1/MNZ_t$ and sonication time is shown in Fig. 21 with K_{obs} values from the slope.

The mechanism of degradation of MNZ was investigated by subjecting the experimental data to Langmuir-Hinshelwood (L-H) model shown in Eq. (4)

$$\frac{1}{K_{obs}} = \frac{1}{K_c K_{LH}} + \frac{1}{K_c} MNZ_O \qquad \ldots(4)$$
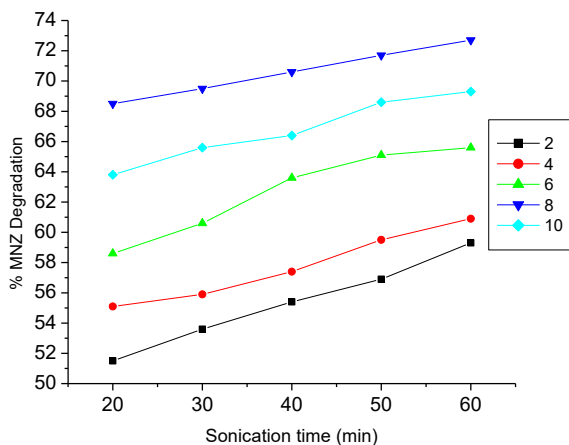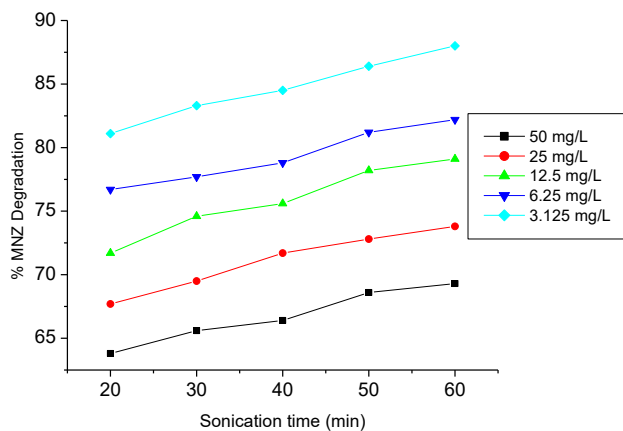
Where K_{obs} is the rate constant (min^{-1}), K_c is the surface rate of reaction constant $(mg.Lmin^{-1})$ and K_{LH} is the L-H adsorption equilibrium constant $(L.mg^{-1})$. The plot of L-H kinetic and R^2 values is shown in Fig. 22 with K_c and K_{LH} values of 1.486×10^{-1} $(mg.Lmin^{-1})$ and 8.790×10^{-2} $(L.mg^{-1})$.

Proposed Reaction Mechanism for MNZ

US only

$$H_2O +)))) \rightarrow OH^* + H^* \qquad \ldots(5)$$

$$H_2O + H \rightarrow OH^* + H_2 \qquad \ldots(6)$$

$$O_2 + H^* \rightarrow HO_2^* \qquad \ldots(7)$$
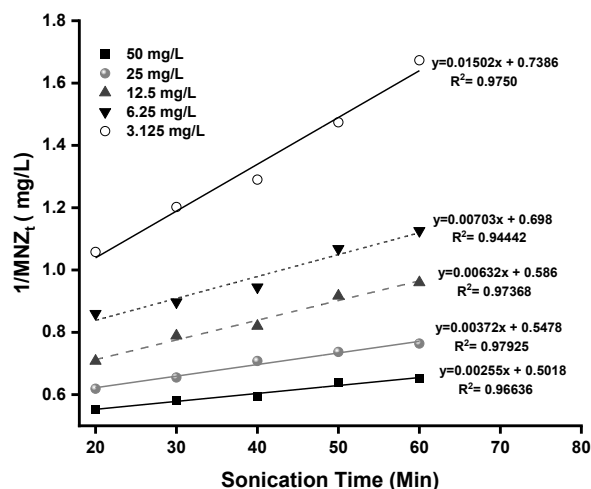

Fig. 21: Plot of 1/MNZt and sonication time for pseudo-second-order kinetic model.

Fig. 19: Influence of pH and sonication time on MNZ removal.

Fig. 20: Influence of initial concentration and sonication time on MNZ removal.
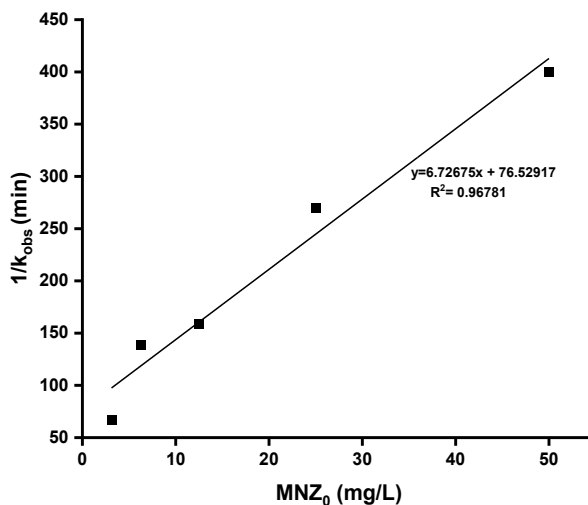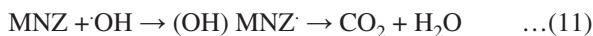

Fig. 22: L-H kinetic plot of MNZ removal.

US/H$_2$O$_2$

H$_2$O$_2$ was decomposed to form reactive radicals in equations (8-10)

$$H_2O_2 +)))) \rightarrow OH^* + OH^* \qquad \ldots(8)$$

$$H_2O_2 + O_2 +)))) \rightarrow 2HO_2 \qquad \ldots(9)$$

$$H_2O_2 + OH^* \rightarrow HO_2^* + H_2O \qquad \ldots(10)$$

US/n-ZnO/H$_2$O

$$MNZ + OH \rightarrow (OH) MNZ^. \rightarrow CO_2 + H_2O \qquad \ldots(11)$$
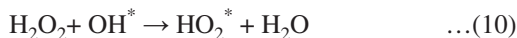
Degradation of MNZ Contained in Aquaculture Effluent

The experimental conditions such as 20% amplitude, 5 mL 2% H$_2$O$_2$, 0.02g n-ZnO, and 60 min sonication time were applied for MNZ degradation in aquaculture effluent. The percentage of COD removal achieved for MNZ in aquaculture effluent was 62.6%, 89.8%, and 98.5% for US only, US/n-ZnO and US/n-ZnO/H$_2$O$_2$ systems and is shown in Fig. 23.

CONCLUSION AND RECOMMENDATIONS

In this study, a stable and effective metal oxide nanoparticle with good antibacterial properties was synthesized and calcined at 500°C. The synthesized n-ZnO depicts a hexagonal structure with an average particle size of 71.48 nm. At 500°C, an absorption peak for the Zn-O bond was observed at 467.21 cm^{-1}, and a well-crystalline zincite was achieved with a surface area of 8.58 m^2.g^{-1} which indicates that n-ZnO is a promising catalyst that is viable for remo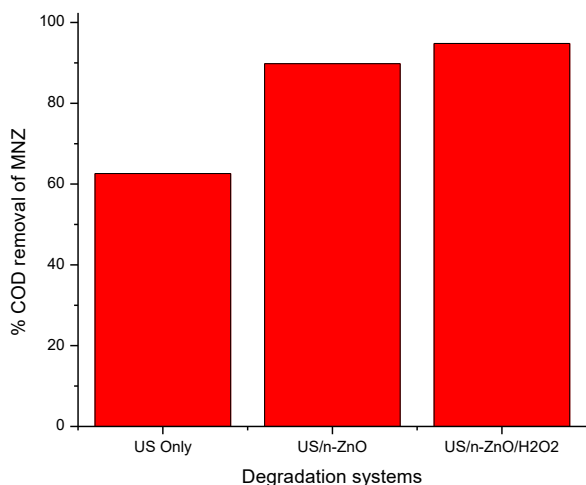ving antibiotics from wastewater. MNZ-formulated aquaculture effluent was subjected to US only, Us/n-ZnO, and US/n-ZnO/H$_2$O$_2$ systems. With the introduction of 0.02 g n-ZnO, 5 mL of 2% H$_2$O$_2$, 20% ultrasonic amplitude and 50 mg.L^{-1} MNZ aqueous solution, the percentage COD removal followed the trend 62.6%, 89.8% and 98.5% for US only, US/n-ZnO and US/n-ZnO/ H$_2$O$_2$ systems. The available active sites of n-ZnO and the hydroxyl radicals generated from H$_2$O$_2$ and that of the sonicator have improved the degradation efficiency. Pseudo-second-order kinetic best fit the degradation process of MNZ and the mechanism of degradation followed the Langmuir-Hinshelwood model. The discharge of metronidazole contained in aquaculture effluent can best be removed by subjecting the effluent to US/n-ZnO/H$_2$O$_2$ system. Other advanced oxidation processes can be explored for further studies.

REFERENCES

Aremu, O.H., Akintayo, C.O., Naidoo, E.B., Nelana, S.M. and Ayanda, O.S. 2021. Synthesis and applications of zinc oxide nanoparticles-A review. Int. J. Environ. Sci. Technol., 16: 1-20.

Ayanda, O.S. Aremu, O.H. Akintayo, C.O. Sodeinde, K.O, Igboama, W.N. Osegbe, E.O. Nelana, S.M. (2021). Sonocatalytic degradation of amoxicillin from aquaculture effluent by zinc oxide nanoparticles. Environ. Nanotechnol. Monit. Manag., 16: 100513.

Balarak, D., Igwegbe, C.A. and Onyechi, P.C. 2019. Photocatalytic degradation of metronidazole using BIOI-MWCNT composites: Synthesis, characterization and operational parameters. Sigma Journal of Engineering and Natural Sciences, 37(4): 1235-1249.

Bian, D., Guo, Y. and Zao, Y., 2017. Influence of zinc oxide on corrosion resistance of alumina-based chemically bonded ceramic coatings. Russ. J. Appl. Chem., 89: 2091-2094.

Calamari, D., Zuccato, E., Castiglioni, S., Bagnati, R. and Fanelli, R. 2003. Strategic survey of therapeutic drugs in the rivers Po and Lambro in Northern Italy. Environ. Sci. Technol., 37: 1241-1248.

Cordero, T., Chovelon, J.M., Duchamp, C., Ferronato, C. and Matos, J. 2007. Surface nano-aggregation and photocatalytic activity of TiO$_2$ on H-type activated carbons. Appl. Catal. B, 73: 227–235.

Cunningham, V.L. 2004. Special Characteristics of Pharmaceuticals Related to Environmental Fate. In Pharmaceuticals in the Environment. Springer Berlin Heidelberg, Berlin, Germany, pp. 13–34.

Das, J. and Dhua, M. 2014. UV-Spectrophotometric assay method development and validation of metronidazole in bulk and tablet formulation. Journal of Pharm Sci Tech, 3(2): 106-109.

El-Kemary, M., El-Shamy, H. and El-Mehasseb, I. 2010. Photocatalytic degradation of ciprofloxacin drug in water using ZnO nanoparticles, J. Lumin., 130(12): 2327-2331.

Felis, E., Kalka, J., Sochacki, A., Kowalska, K., Bajkacz, S., harnisz, M. and Korzeniewska, E. 2020. Antimicrobial pharmaceuticals in the aquatic environment-Occurrence and environmental implications. Europ. J. Pharma., 886: 172813.

Forouzesh, M., Ebadi, A. and Aghaeinejad-Meybodi, A. 2018. Degradation of metronidazole antibiotic in an aqueous medium using activated carbon as a persulfate activator. Sep. Purif. Technol., 16: 1-31.

Habibi, A., Belaroui, L.S., Bengueddach, A., Galindo, A.L. Díaz, C.I.S. and Peña, A. 2018 Adsorption of metronidazole and spiramycin by an Algerian palygorskite. Effect of modification with tin, Micropor. Mesopor. Mater., 268: 293-302.

Hemati Borji, S., Nabizadeh, R., Mahvi, A.H. and Javadi, A.H .2010. Photocatalytic degradation of phenol in aqueous solutions by

Fig. 23: Degradation efficiency by COD removal of MNZ from aquaculture effluent using US only, US/n-ZnO, and US/n-ZnO/ H$_2$O$_2$ systems.

Fe (III)-doped TiO2/ UV process. Iran. J. Health Environ., 3: 369-380.

Hu, Y., Wang, G., Huang, M., Lin, K., Yi, Y., Fang, Z., Li, P. and Wang, K. 2017. Enhanced degradation of metronidazole by heterogeneous sono-Fenton reaction coupled ultrasound using Fe_3O_4 magnetic nanoparticles. Environ. Technol., 11: 1-22.

Ismail, M.A., Taha, K.K., Modwi, A. and Khezami, L. 2018. ZnO nanoparticles: Surface and x-ray profile analysis. J. Ovonic Res., 14(5): 381-393.

Jury, K.L., Vancov, T., Stuetz, R.M. and Khan, S.J. 2010. Antibiotic resistance dissemination and sewage treatment plants. Curr. Res. Technol. Educ. Top. Appl. Microbiol. Microbial Biotechnol., 2: 509-510.

Kayani, Z.N., Saleemi, F. and Batool, I. 2015. Effect of calcination temperature on the properties of ZnO NPs. Appl. Phys. A, 119(2): 713-720

Kołodziejczak-Radzimska, A., Markiewicz, E. and Jesionowski, T. 2012. Structural characterization of ZnO particles obtained by the emulsion precipitation method. J. Nanostruct., 3: 1-9.

Landers, T.F., Cohen, B., Wittum, T.E. and Larson, E.L. 2012. A review of antibiotic use in food animals: perspective, policy, and potential. Pub. Health Rep., 127(1): 4-22.

Ma, H., Williams, P.L. and Diamond, S.A. 2013. Ecotoxicity of manufactured ZnO nanoparticles-a review. Environ. Pollut., 172: 76-85.

Malakootian, M., Olama, N. and Dehghani, M. 2019. Photocatalytic degradation of metronidazole from aquatic solution by TiO_2 doped Fe3+ nano-photocatalyst. Int. J. Environ. Sci. Technol., 16(8): 4275-4284.

Mallika, N.A., Reddy, A.R. and Reddy, K.V. 2015. Annealing effects on the structural and optical properties of ZnO NPs with PVA and CA as chelating agents. J. Adv. Ceramics, 4(2): 123-129.

Manyi-Loh, C., Mamphweli, S., Meyer, E. and Okoh, A. 2018. Antibiotic use in agriculture and its consequential resistance in environmental sources: potential public health implications. Molecules, 23(4): 795.

Moussavi, G., Alahabadi, A., Yaghmaeian, K. and Eskandari, M. 2013. Preparation, characterization, and adsorption potential of the NH_4Cl-induced activated carbon for the removal of amoxicillin antibiotic from wastewater. Chemical Engineering Journal, 217: 119-128.

Petrie, B., Barden, R. and Kasprzyk-Hordern, B. 2015. A review on emerging contaminants in wastewaters and the environment: current knowledge, understudied areas, and recommendations for future monitoring, Water Res., 72: 3-27.

Qiao, J., Zhang, H., Li, G., Li, S., Qu, Z., Zhang, M., Wang, J. and Song, Y. 2018. Fabrication of a novel Z-scheme SrTiO3/Ag2S/CoWO4 composite and its application in sonocatalytic degradation of tetracyclines. Sep. Purif. Technol., 211: 843-856.

Saif-Aldin, K., Al-Hariri, S. and Ali-Nizam, A. 2020. Zinc oxide nanoparticles synthesis without organic solvents with ultrasonic wave assistance. Chem. Res. J., 5(3): 6-13.

Sharifpour, E., Khafri, H.Z., Ghaedi, M., Asfaram, A. and Jannesar, R. 2018. Isotherms and kinetic study of ultrasound-assisted adsorption of malachite green and $Pb2^+$ ions from aqueous samples by copper sulfide nanorods loaded on activated carbon: experimental design optimization. Ultrason. Sonochem., 40: 373-382.

Yang, Z., Lai, A., Chen, H., Yan, Y., Yang, Y., Zhang, W. and Wan, L. 2019. Degradation of metronidazole by dielectric barrier discharge in an aqueous solution. Front. Environ. Sci. Eng., 13(3): 1-9.

Zak, A.K., Abd Majid, W.H., Wang, H. Z., Yousefi, R., Golsheikh, A.M. and Ren, Z. F. 2013. Sonochemical synthesis of hierarchical ZnO nanostructures. Ultrason. Sonochem., 20(1): 395-400.